JOURNAL OF MATERIALS SCIENCE 30 (1995) 1225–1232

Dynamic mechanical properties of carbon–carbon composites

WEN-CHI CHANG*, NYAN-HWA TAI‡, CHEN-CHI M. MA*‡§
Institute of Chemical Engineering and ‡Materials Science Center, National Tsing Hua University, Hsin-Chu, Taiwan 30043

The dynamic mechanical analysis (DMA) method was utilized to investigate the dynamic mechanical properties of the carbon–phenolic composite, and of carbon–carbon (C/C) composites carbonized at 1000 °C, and graphitized at 2200 °C. The measurements were performed in the temperature range 50–450 °C. Results show that the carbon–phenolic composite has the highest storage modulus, while the carbonized C/C composites possess higher storage modulus than the graphitized C/C composite. The storage moduli of carbonized and graphitized C/C composite do not change significantly in the test temperature range. The tan δ, loss factor, of carbonized C/C composites increases 59.5% during the tests from 50 to 450 °C, and that of the graphitized C/C decreases 9.74% in the same temperature range; graphitized C/C shows the highest tan δ at 50 °C. The carbon–phenolic composite shows a damping peak at 250 °C, which is probably due to the transition from glassy state to rubbery state of the phenolic matrix. The higher tan δ of the graphitized C/C composite may be due to matrix graphitization, fibre–matrix debonding and crack formation, which were observed on the micrographs.

1. Introduction

The carbon–carbon (C/C) composite is one of the structural materials used for high temperature application in the aeronautic and aerospace industry [1–3]. The manufacturing processes for C/C composites involve carbonization of the resin matrix precursor followed by a graphitization treatment, which results in improved density, thermal conductivity and crystallinity of the C/C composites [4–7].

For the materials used in structure applications, it is important to understand the mechanical properties of the materials. Dynamic mechanical analysis is commonly adopted to measure the deformation of a material in response to vibration forces. The dynamic storage modulus, loss modulus and mechanical damping (or internal friction) can be determined from dynamic mechanical analysis. The dynamic storage modulus (or elastic modulus) is one of the most basic mechanical properties, and it is of great importance in any structural application [8]. Damping is another important material property for structural application, and it is one of the most sensitive indicators of molecular motion in material. A high damping rate results in some advantages and drawbacks in real applications. For instance, a high damping rate (or internal friction) is essential in decreasing the effect of undesirable vibration, thus reducing the amplitude of resonance vibrations to prevent all kinds of vibrational amplifications; however, damping generates heat and thus degrades material more rapidly [9–12]. Therefore, it is of importance to take into account mechanical damping in engineering applications.

Bidde and Johnson [13] utilized a dynamic mechanical analyser to study the mechanical properties of two-dimensional carbon–carbon composites over the temperature range from ambient to 500 °C. Reproducibility of the storage modulus has been shown to be within 5% at any one temperature over the entire temperature range. They concluded that the pitch matrix samples show a higher modulus than that of the chemical vapour deposition (CVD) samples in all cases studied. Furthermore, all these specimens show a decrease in modulus with increasing temperature up to the analysis limit of 500 °C.

In this study, the dynamic mechanical properties of carbon–phenolic, C/C composites carbonized at 1000 °C, and C/C composites graphitized at 2200 °C were investigated. The dynamic storage modulus, loss modulus and tan δ (loss factor) of these composites were measured under oscillatory load between 50 and 450 °C. The microstructure of the composites was studied by X-ray diffraction (XRD) and optical microscopy (OM).

2. Experimental procedure

2.1. Sample preparation

The composite laminates were fabricated by wet dipping, followed by a hand lay-up method. The laminates consist of six layers of carbon fabric impregnated with phenolic resin. The materials used in this study are summarized in Table I. The impregnated

§To whom all correspondence should be addressed.

TABLE I Materials used in this study

Specification	Code	Supplier
Resin		
Resole type phenolic resin PH = 8.0–8.5 Solid content 62% Viscosity at 25 °C = 100–250 cps	PF-650	Chung-Chun Plastics Co., Ltd, Taiwan
Carbon fibre		
Plain weave cloth 200 g cm^{-2} Fibre diameter = 7.0 μm	TR-30K	Mitsubishi Rayon Co., Ltd, Japan

fabrics were placed in a picture frame mould and then compression moulded at 150 °C under 17.25 MPa pressure. The resulting carbon–phenolic composite laminates were post-cured in an air circulation oven at 150 °C for 36 h. Test specimens were cut from the laminates and were machined to 50×10×1 mm with a diamond saw cutter under water cooling.

2.1.1. Carbonization

The carbonization process was performed at 1000 °C on a Linberg high temperature tube furnace Model-54434 under argon atmosphere at a constant gas flow rate of 100 cm^3 min^{-1} with a heating rate 30 °C h^{-1}.

2.1.2. Graphitization

The graphitization process was carried out at 2200 °C in a graphite furnace produced by Thermal Technology Inc., Model 1000–3060-FP20 under an argon atmosphere at a constant flow rate of 100 cm^3 min^{-1} with a heating rate 3 °C min^{-1}.

2.2. Dynamic mechanical properties test

The DMA tests were carried out using a Perkin Elmer DMA 7 between 50 and 450 °C by a three point bending method. The sample was placed into a furnace which provided a programmed temperature environment during test. The storage modulus, loss modulus, and tan δ were calculated from the computer program in the test instrument.

2.3. Static mechanical properties

Static flexural strength and modulus were measured by a three point bending method, with a span to depth ratio of 40. The test speed used was 1.3 mm min^{-1}. All tests were performed on an Instron testing machine Model 4201. Interlaminar shear strength (ILSS) was measured, with a span to depth ratio of 5 to 1. The test results are summarized in Table II.

2.4. Microstructure evaluation

The morphology of the carbonized composites was analysed with an optical microscope (OM). X-ray diffraction (XRD) was utilized to investigate the molecular structure rearrangement in the composite after different heat treatments. All specimens were analysed by copper radiation, using a computer controlled powder diffractometer, at a speed of 4 min^{-1} at 40 kV and 30 mA.

The d-spacing, $d002$, was calculated using Bragg's equation [14]

$$n\lambda = 2d\sin\theta \quad (1)$$

and the average crystallite dimension in the c-direction (stacking height of crystallite, L_c) was calculated according to the Scherrer equation [14]

$$L_c = \frac{0.9\lambda}{(\Delta 2\theta)\cos\theta} \quad (2)$$

where n is an integer, λ the X-ray wavelength, θ the Bragg angle of the (002) reflection peak and $\Delta 2\theta$ the half-height width of the diffraction intensity distribution (measured in radians).

3. Results and discussion

3.1. Carbon–phenolic composite

The storage modulus, loss modulus and tan δ of the carbon–phenolic composite obtained from DMA testing are shown in Fig. 1. The storage modulus decreases quickly at temperatures over 200 °C, and a reflection point at 280 °C is observed. Once the test temperature exceeds 350 °C, the phenolic resin decomposes and some volatile byproducts diffuse out. To avoid contaminating the test instrument with the volatile byproducts, the test was stopped at 350 °C. The storage modulus of the carbon–phenolic composites decreased by 20% when the temperature was raised from 200 to 280 °C. The decrease of storage modulus above 200 °C is due to the glassy transition behaviour of the phenolic resin, since the polymer lost its rigidity once the environmental temperature exceeded its glassy transition temperature, T_g. Once the temperature exceeds 280 °C, the crosslinking density of

TABLE II Physical and static mechanical properties of composites in this study

	Carbon–phenolic composite	Carbonized C/C composite	Graphitized C/C composite
Density (g cm^{-3})	1.553 ± 0.017	1.410 ± 0.012	1.445 ± 0.002
Open porosity (%)	2.3 ± 0.5	11.0 ± 1.6	12.2 ± 1.0
Flexural strength (MPa)	380 ± 2.5	136.6 ± 11.5	111.0 ± 20.6
Flexural modulus (MPa)	108.1 ± 4.5	47.8 ± 3.5	26.51 ± 4.1
ILSS (MPa)	23.1 ± 1.4	7.5 ± 0.5	6.8 ± 0.6
Shrinkage (%)	–	1.44 ± 0.01	4.31 ± 0.75

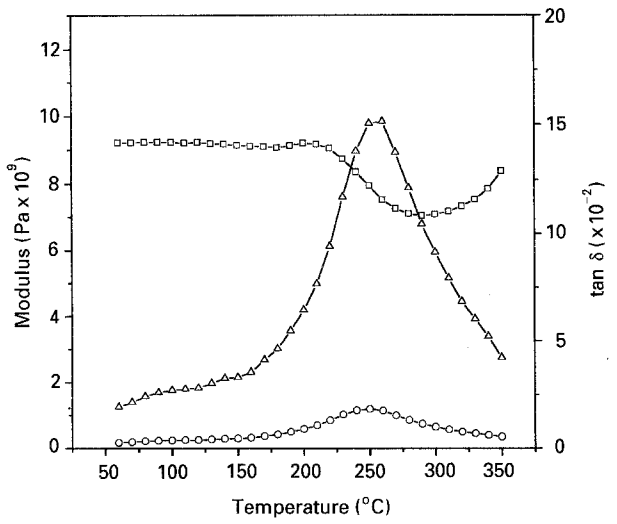

Figure 1 DMA curves for non-pyrolysis carbon–phenolic composites at a heating rate of 10 °C min^{-1}: (△) tan δ, (□) storage modulus, and (○) loss modulus.

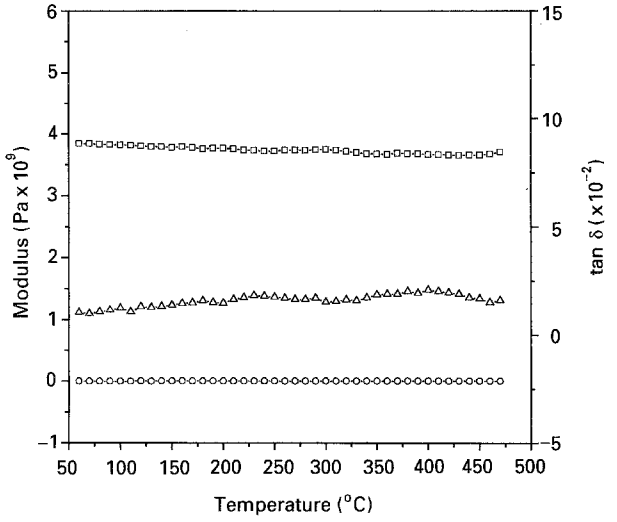

Figure 2 DMA curves for 1000 °C carbonized C/C composites at a heating rate of 10 °C min^{-1}: (△) tan δ, (□) storage modulus, and (○) loss modulus.

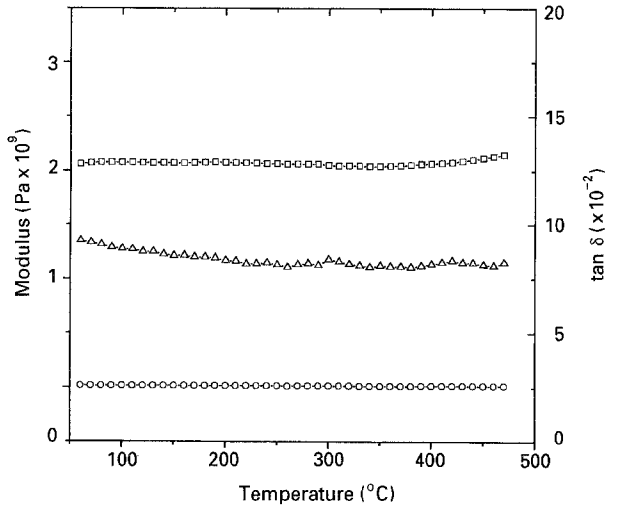

Figure 3 DMA curves for 2200 °C graphitized C/C composites at a heating rate of 10 °C min^{-1}: (△) tan δ, (□) storage modulus, and (○) loss modulus.

phenolic resin is increased due to the oxidation reaction at high temperatures [15]. The increase of crosslinking density enhances the Young's modulus of phenolic resin, consequently, increasing the dynamic storage modulus of the composites.

The tan δ curve possesses a damping peak at 250 °C. The damping peak is associated with the partial loosening of the phenolic resin structure, so that small chain segments can move. Tan δ decreases when the temperature exceeds 250 °C, where a crosslinking reaction may occur. Phenolic resin reacts with oxygen supplied from air, or from the phenolic resin itself, to form an ether linkage, which will increase the crosslinking density of the cured phenolic resin. The increase of crosslinkage restricts the motion of the molecular chain, therefore, enhancing the storage modulus and storage energy of the segment. Since the molecular chains are restricted in movement, the value of tan δ decreases and damping of the carbon–phenolic composite at temperatures over 250 °C is reduced sharply. The tendency of the loss modulus curve is similar to the tan δ curve.

3.2. Carbon–carbon composites

The DMA curves of the carbonized and graphitized C/C composites are shown in Figs 2 and 3, respectively. The storage modulus of the carbonized C/C composites decreases slightly from 3.844 to 3.656 GPa in the temperature range 50–450 °C, and tan δ increases slightly from 0.0106 to 0.0168 in the test temperature range. While the storage modulus of the graphitized C/C composite increases from 2.061 to 2.117 GPa, tan δ decreases from 0.0924 to 0.0814 in the test temperature range. The linear regression method was utilized to analyse the experimental data and to study the dependency of storage modulus, loss modulus and tan δ on temperature. Based upon the results shown in Table III, it was found that the slope of the linear regression equation of the storage modulus is negative for the carbonized C/C composite, and is positive for the graphitized C/C composite. The absolute values of the slopes are quite small, and the rate of change of the storage modulus from 50 to 450 °C is only 5% for carbonized and 2.7% for graphitized C/C composites. Standard derivation of the DMA test is within 5%. It can be seen that the storage modulus does not change significantly with temperature between 50 and 450 °C. The effect of temperature on tan δ is more significant than storage modulus. As shown in Table III, variation of tan δ is 58.5% for the carbonized C/C composite, and 11.9% for the graphitized C/C composite. The reason for the influence of temperature on storage modulus and tan δ of C/C composites is still ambiguous. It may be due to the different microstructure of the carbonized and graphitized C/C composites.

Fig. 4 compares the storage modulus of the three composites investigated in this study. At 50 °C, the storage modulus is 9.216 GPa for carbon–phenolic composites, 3.844 GPa for carbonized C/C composites, and 2.061 GPa for graphitized C/C composites. The dynamic storage modulus decreases significantly as the heat treatment temperature increases. Static

TABLE III The result of linear regression treatment on the dynamic mechanical properties of carbonized and graphitized C/C composites: $Y = A + B \times X$

	A	B	C^a
Storage modulus of carbonized C/C (GPa)	3.86	−4.61E-4	−4.80%
Storage modulus of graphitized C/C (GPa)	2.06	4.29E-5	+0.82%
Loss modulus of carbonized C/C (GPa)	4.34E-3	6.13E-6	+52.70%
Loss modulus of graphitized C/C (GPa)	0.0184	−4.10E-6	−8.79%
Tan δ of carbonized C/C	0.0112	1.81E-5	+59.50%
Tan δ of graphitized C/C	0.0894	−2.15E-5	−9.74%

[a] C, the percentage change of Y between 50 and 450 °C, $C = (Y_{450\,°C} - Y_{50\,°C}/Y_{50\,°C}) \times 100\%$.

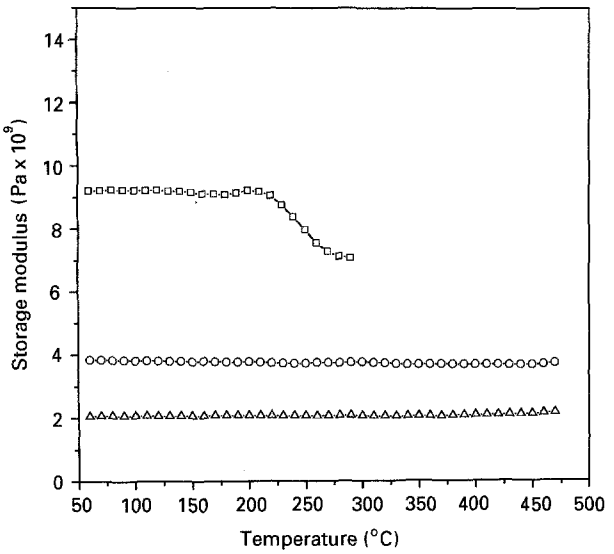

Figure 4 The storage modulus curves for the three composites tested at a heating rate of 10 °C min^{-1}: (□) non-pyrolysed, (○) carbonized, and (△) graphitized composite.

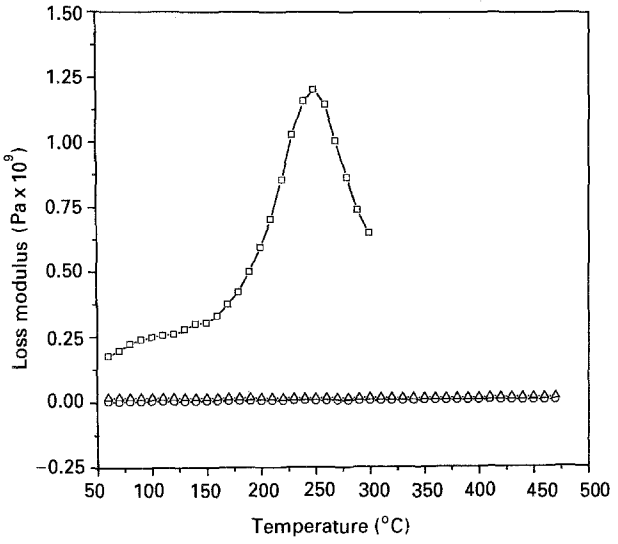

Figure 6 The loss modulus curves for the three composites tested at a heating rate of 10 °C min^{-1}: (□) non-pyrolysed, (○) carbonized, and (△) graphitized composite.

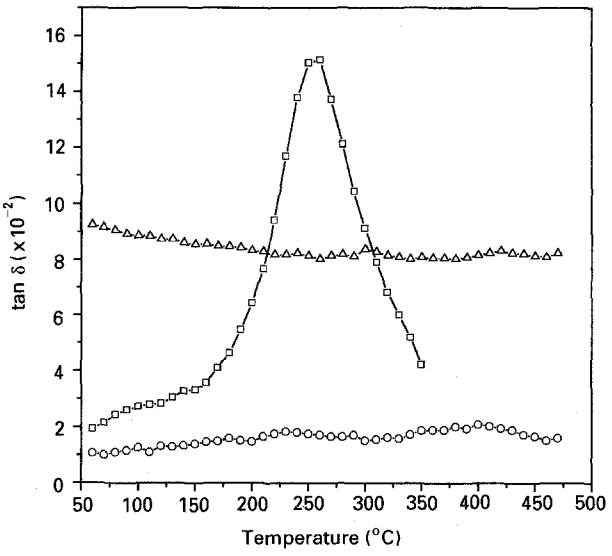

Figure 5 The tan δ curves for the three composites tested at a heating rate of 10 °C min^{-1}: (□) non-pyrolysed, (○) carbonized, and (△) graphitized composite.

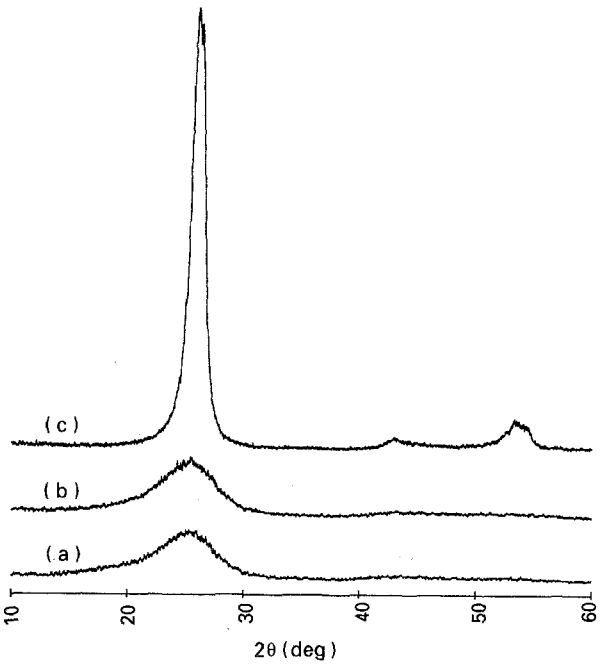

Figure 7 XRD patterns for the three composites: (a) carbon–phenolic composite, (b) carbonized C/C composite, and (c) graphitized C/C composite.

flexural strength and modulus also decrease as the heat treatment temperature increases. As indicated in Table II, flexural strength decreases from 380 to 136.6 MPa after carbonization, and decreases to

TABLE IV The results of XRD

	Carbon–phenolic composite	Carbonized C/C composite	Graphitized C/C composite
2θ (deg)	25.21	25.23	26.10
Peak intensity (count)	754	847	3464
Half-width (deg)	6.0	5.5	1.37
d_{002} (nm)[a]	0.3530	0.3527	0.3411
L_c (nm)[b]	1.46	1.60	64.6

[a] The d-spacing is calculated by Bragg's equation [14].
[b] The stacking height is calculated by Scherrer's equation [14].

110 MPa after graphitization treatment. The shift of the dynamic storage modulus and static flexural modulus to a lower value is due to the loss of stiffness of the composite, which may be attributed to the formation of cracks and pores, fibre–matrix debonding and fibre breakage of the composite during high temperature treatment. Kupkova [16] utilized a theoretical analysis method to correlate porosity with elastic modulus for brittle material systems, and showed that the elastic modulus reduced with increasing porosity. The porosity of the C/C composite increases from 2.3 to 11% after carbonization treatment, to 12.2% after graphitization treatment. Microstructural changes will be discussed later.

Figs 5 and 6 compare tan δ and loss modulus of these three composites. As discussed previously, the tan δ curve of the carbon–phenolic composite shows a peak around 250 °C. Tan δ of the carbonized C/C composite decreases linearly with temperature, whereas it increases linearly between 50 and 450 °C for the graphitized C/C composite. It is interesting to note that tan δ of the graphitized C/C composite is higher than that of the carbonized C/C composite in the test temperature range. The high damping of the graphitized C/C composite may be attributed to the following mechanisms.

1. Increase of friction between graphite layers, after graphitization treatment. The carbon atom could have been rearranged to obtain a more regular layer structure during graphitization, hence increasing the crystallinity of the C/C composite, as shown in Fig. 7.

2. Excess damping near the fibre–matrix interface, due to thermal stress in graphitization process may reduce the interlaminar shear strength of the C/C composite from 7.5 to 6.8 MPa, as shown in Table II. When the bonding strength of the laminate is reduced, there is less restriction for layers to move or vibrate, hence the damping of the composite is increased due to the existence of voids or defects in the fibre–matrix interface.

3. More pores and cracks are generated after graphitization treatment, providing more free space to oscillate, generating excess damping.

3.3. Microstructure

The X-ray diffraction peaks of the composites are shown in Fig. 7. The Bragg diffraction angle, peak intensity, peak half-width, d-spacing and stacking height are listed in Table IV. The carbon–phenolic and carbonized C/C composite show the same type of diffraction pattern, exhibiting a broad peak at $2\theta = 25.21$ and 25.23, respectively. For the graphitized C/C composite, the diffraction pattern shows a sharp peak at $2\theta = 26.10$. The peak intensity of the graphitized C/C composite is much higher than that of the carbonized C/C composite and carbon–phenolic composite, whereas the graphitized C/C composite shows the narrowest peak half-width among these three composites. The d-spacings calculated from Bragg's equation are 0.3530 and 0.3527 nm for the carbon–phenolic and carbonized C/C composites, respectively. However, the graphitized C/C composite has an average d-spacing of 0.3411 nm, which is the closest to a perfect graphite crystallite of 0.335 nm [5]. From the stacking height of the graphite layers, L_c, calculated from Scherrer's equation [14], it is found that the stacking height of the graphitized C/C composite is 64.6 nm, which is much higher than those of the carbonized C/C (1.6 nm) and the carbon–phenolic (1.46 nm) composites. The average crystallite is increased rapidly after graphitization treatment.

The broad shape of the diffraction peaks for the carbon–phenolic and carbonized C/C composite is due to the non-crystalline characteristic of the bulk matrix, and the peaks are contributed to primarily by ordered carbon layers within the carbon fibres. Since the crystallinity of carbon fibres does not change up to a treatment temperature of 1000 °C, the diffraction curve of the composite does not change significantly after carbonization treatment. Upon further heat treatment to 2200 °C, as shown in Fig. 7, a sharper pattern is formed, and a shift of the pattern to the higher angle side is observed. Fig. 8 shows the pattern on a larger scale, it is found that the pattern is not symmetric. The pattern possess two small peaks at $2\theta = 26.38$ and 26.06, which correspond to d-spacings of 3.376 and 3.420 nm, respectively. The peak at 26.38 2θ is attributed to the graphitic carbon, with a d-spacing 3.376 nm, and the other is the peak of turbostatic carbon, with a d-spacing of 3.42 nm.

3.4. Morphology

Fig. 9 is an optical micrograph of the as-fabricated carbon–phenolic composite; no significant crack can be observed. However, some small pores in the carbon–phenolic composite, as shown in Fig. 10, can be found. The porosity measured is 2.3%.

Cracks in carbonized C/C composites can be seen, as shown in Figs 11 to 14. The cracks can be catalogued as: (a) transverse cracks, the large cracks

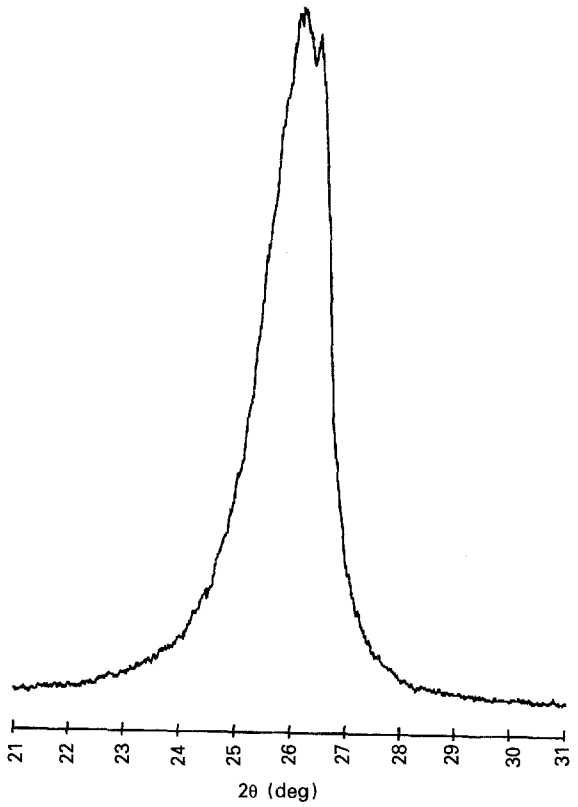

Figure 8 XRD pattern for graphitized C/C composite with a larger scale.

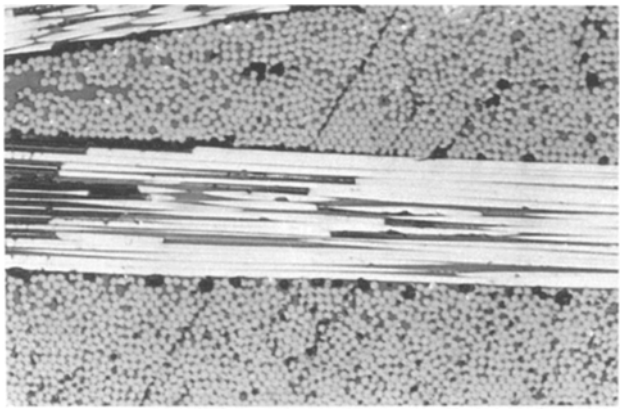

Figure 9 Optical micrograph of the carbón–phenolic composite (× 200).

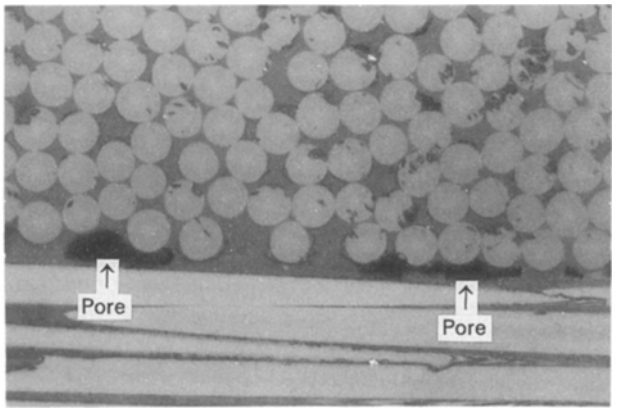

Figure 10 Optical micrograph of the carbon–phenolic composite (× 1000).

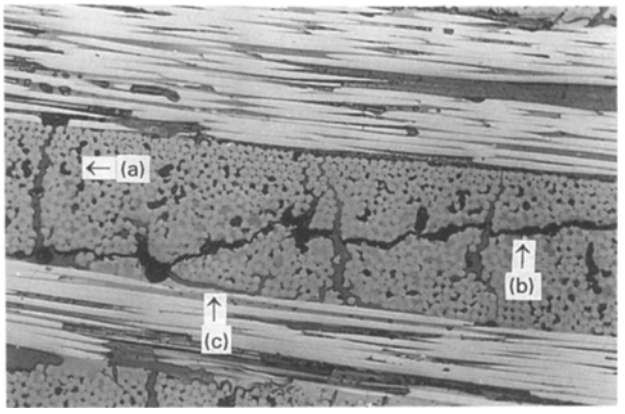

Figure 11 Optical micrograph of the carbonized C/C composite (× 200): (a) transverse crack, (b) longitudinal crack, and (c) delamination crack.

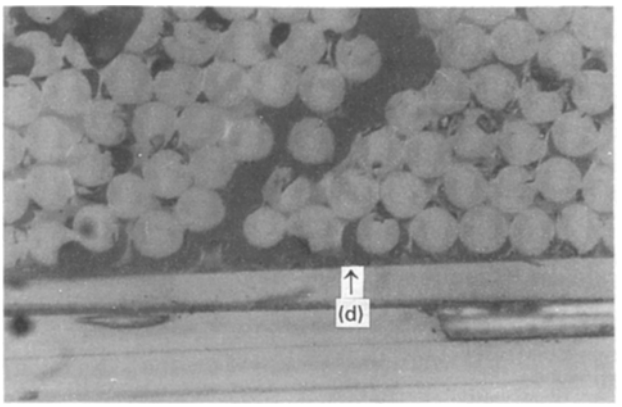

Figure 12 Optical micrograph of the carbonized C/C composite (× 1000): (d) indicates fibre–matrix debonding.

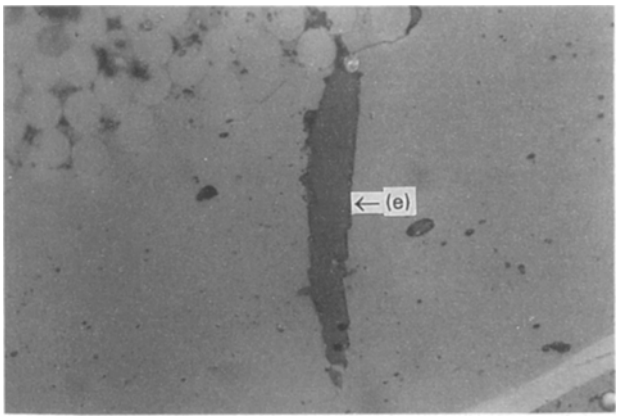

Figure 13 Optical micrograph of carbonized C/C composite (× 1000): (e) indicates crack in matrix rich region.

between laminate layers (Fig. 11); (b) longitudinal cracks, i.e. cracks within the laminar layer bundle (Fig. 11); (c) delamination cracks, the gap type crack along laminate layers (Fig. 11); (d) fibre–matrix debonding, the smaller cracks in the fibre–matrix interface region (Fig. 12); (e) matrix cracks, the cracks in the matrix rich region (Fig. 13); and (f) fibre breakage, the breakage of reinforced carbon fibre at the end of

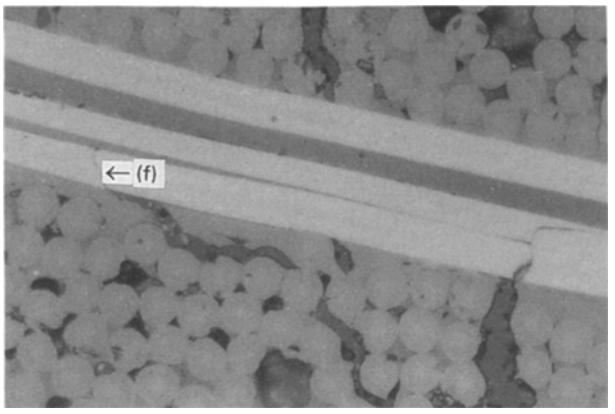

Figure 14 Optical micrograph of carbonized C/C composite (× 1000): (f) indicates fibre breakage.

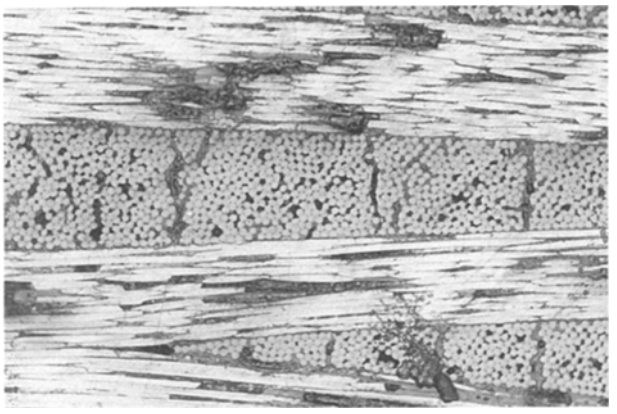

Figure 15 Optical micrograph of graphitized C/C composite (× 200).

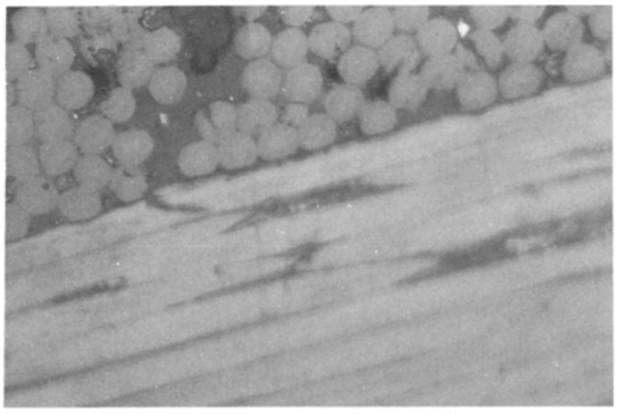

Figure 16 Optical micrograph of graphitized C/C composite (× 1000).

a transverse crack (Fig. 14). The porosity is increased from 2.3 to 11.0% after carbonization treatment.

Figs 15 and 16 are micrographs of graphitized composites. The types of cracks and defects in the graphitized C/C composite are similar to those of carbonized C/C composites. More transverse cracks are observed in the graphitized C/C composite than in the carbonized C/C composite. The porosity of C/C composite increases from 11% to 12.2% after graphitization. This increase in porosity is due to the formation of more cracks, attributed to thermal stresses and volatile species generated during graphitization treatment. It is worth noting the change in shape of the carbon fibre cross-section from circular to hexagonal after graphitization, since the heat treatment temperature of the as-received carbon fabrics is only 1000 °C.

4. Conclusions

The dynamic storage modulus, loss modulus and tan δ were studied for carbon–phenolic, carbonized C/C and graphitized C/C composites. The carbon–phenolic composite showed the highest storage modulus between 50 and 300 °C. The storage modulus of the carbon–phenolic composite decreased from 200 °C due to the glassy transition behaviour of the phenolic resin. The behaviour also resulted in a damping peak of the tan δ curve at 250 °C. The storage modulus of the carbonized C/C composite was lower than that of the carbon–phenolic composite, and higher than that of the graphitized composite in the test temperature range; and it was also found that variation in loss modulus between carbonized and graphitized C/C composites is not obvious. Tan δ of the carbonized C/C composite increased 59.5% between 50 to 450 °C, and that of graphitized C/C decreased 9.74% in the same temperature range. The graphitized C/C composite possessed the highest tan δ between 50 and 200 °C, and this was higher than that of the carbonized C/C composite within the entire test temperature range. The lower storage modulus and the higher tan δ value of the graphitized C/C composite, as compared with the carbonized C/C composite, may have been due to graphitization treatment, fibre–matrix debonding and more crack and pore formation in the composite during graphitization treatment.

Acknowledgements

This research was financially supported by the National Science Council, Taiwan, under contract No. NSC-82-0405-E007-523.

References

1. E. FITZER, *Carbon* **25** (1987) 163.
2. G. W. MEETHAM, *J. Mater. Sci.* **26** (1991) 853.
3. E. FITZER and W. HUTTNER, *J. Phys. D: Appl. Phys.* **14** (1981) 347.
4. J. D. BUCKLEY, *Ceram. Bull.* **67** (1988) 364.
5. G. SAVAGE, "Carbon–Carbon Composites" (Chapman & Hall, London, 1993) pp. 137–139.
6. J. D. NAM and J. C. SEFERIS, *Carbon* **30** (1992) 751.
7. H. WEISSHAUS, S. KENIG and A. SIEGMANN, *ibid.* **29** (1991) 1203.
8. S. W. TSAI, "Introduction to Composite Materials" (Technomic Publishing, Wesetport, CT, 1980) pp. 1–24.
9. T. MURAYAMA, "Dynamic Mechanical Analysis of Polymeric Material" (Elsevier Scientific, New York, 1978) pp. 10–35.
10. L. E. NIELSEN, "Mechanical Properties of Polymers and Composites" (Marcel Dekker, New York, 1974) pp. 139–235.
11. M. P. BLAKE and W. S. MITCHELL, "Vibration and Acoustic Measuring Handbook" (Spartan, New York, 1972) pp. 1–15.

12. R. N. HAMME, "Harris Handbook of Noise Control: Vibration Damping" (McGraw-Hill, New York, 1957) pp. 1–10.
13. R. A. BIDDLE and W. L. JOHNSON, III, *Compos. Sci. Technol.* **29** (1987) 239.
14. B. D. CULLITY, "Elements of X-Ray Diffraction", 2nd Edn (Addison-Wesley MA, 1978) p. 102.
15. R. T. CONLEY, *J. Appl. Polym. Sci.* **9** (1965) 1117.
16. M. KUPKOVA, *J. Mater. Sci.* **28** (1993) 5265.

Received 2 February
and accepted 28 June 1994